



# IJSRM

INTERNATIONAL JOURNAL OF SCIENCE AND RESEARCH METHODOLOGY

An Official Publication of Human Journals



Human Journals

Research Article

June 2019 Vol.:12, Issue:4

© All rights are reserved by Silvia Antonia Brandán et al.

## Structures, Reactivities and Vibrational Study of Species Derived from the Adrenergic $A_2$ Receptor Agonist Guanfacine Agent



**Davide Romani<sup>a</sup>, José Ruiz Hidalgo<sup>a</sup>, Maximiliano A. Iramain<sup>a</sup>, Silvia Antonia Brandán<sup>b,\*</sup>**

<sup>a</sup>SST, Servizio sanitario della Toscana, Azienda USL 9 di Grosseto, Via Cimabue, 109, 58100 Grosseto, Italia.

<sup>b</sup>Cátedra de Química General, Instituto de Química Inorgánica, Facultad de Bioquímica. Química y Farmacia, Universidad Nacional de Tucumán, Ayacucho 471, (4000) San Miguel de Tucumán, Tucumán, Argentina.

**Submission:** 26 May 2019

**Accepted:** 31 May 2019

**Published:** 30 June 2019



HUMAN JOURNALS

[www.ijsrm.humanjournals.com](http://www.ijsrm.humanjournals.com)

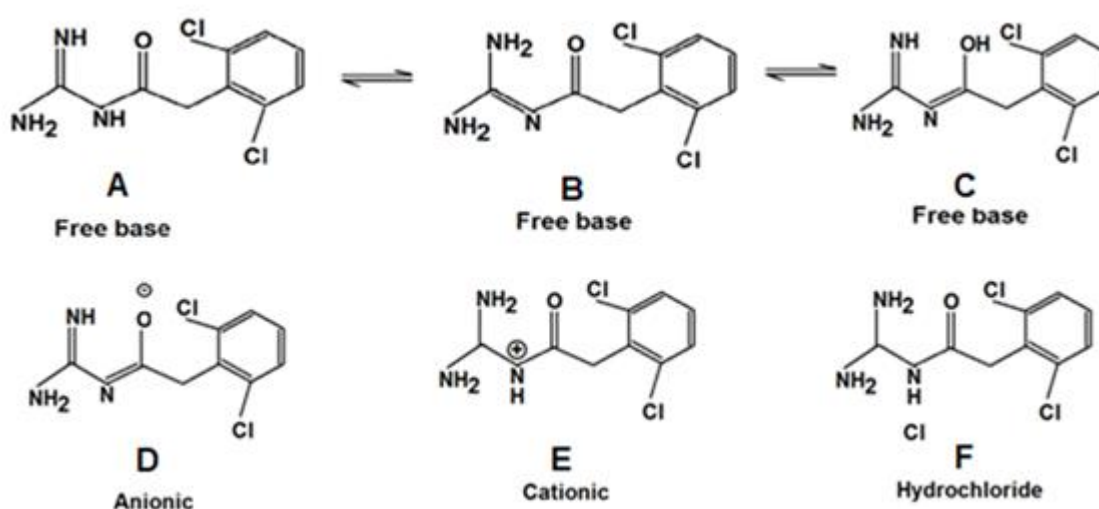
**Keywords:** Guanfacine, solvation energy, force fields, vibrational analysis, DFT calculations

### ABSTRACT

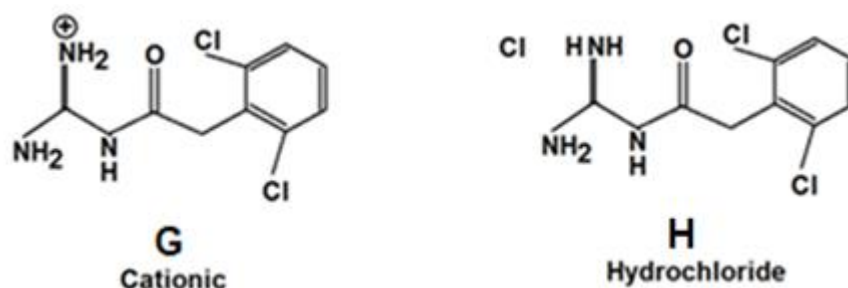
In the present work, eight different species of adrenergic  $\alpha_2$  receptor agonist guanfacine have been theoretically studied in gas phase and in aqueous solution combining hybrid B3LYP/6-31G\* calculations with the Scaled Mechanical Quantum Force Field (SQMFF) methodology and the experimental available infrared and Raman spectra in order to perform their complete vibrational assignments. Hence, the different structures of three tautomeric forms of free base (A, B and C), two cationic (E and G), one anionic (D) and two hydrochloride (F and H) species of that antihypertensive agent were optimized in solution with the Integral Equation F variant Polarised Continuum Method (IEFPCM) and the universal solvation model. The anionic species of guanfacine presents the higher corrected solvation energy with valor of -301,60 kJ/mol, slightly lower than the corresponding to scopolamine alkaloid (-310.34 J/mol) and higher than the corresponding to cocaine alkaloid (-255.24 J/mol). The studies of the frontier orbitals have evidenced that in gas phase, the anionic D species is the most reactive while in solution the hydrochloride H species is the most reactive together with the anionic species. High global nucleophilicity ( $E$ ) and electrophilicity indexes ( $\omega$ ) values have evidenced both cationic species E and G while the lower values of both indexes are predicted for the anionic D species in both media. In addition, the harmonic force fields, force constants and the complete vibrational assignments for the 63, 66, 69 and 72 vibration normal modes expected for the anionic, free bases, cationic and hydrochloride species of guanfacine are respectively reported for first time.

## INTRODUCTION

The compound *N*-(diaminomethylidene)-2-(2,6-dichlorophenyl)acetamide, known as guanfacine, is an adrenergic  $\alpha_2$  receptor agonist used to treatment of arterial hypertension [1-14]. Its pharmacological properties and therapeutic efficacy as antihypertensive agent were reported from long time by Sorkin and Heel [1]. Generally, the form used of this drug is the hydrochloride but the free base, cationic and anionic forms also can be observed in different media. The guanfacine structure as free base was determined from the formation of a copper(II) complex by X-ray crystallography by Tomas *et al* [2]. Hence, this ability of guanfacine to form complexes with different metal is a very important property that could be used to control the concentration levels of diverse metals, such as Cu(II), because the arterial hypertension is one of considerable factors that generate cardiovascular diseases [5,8,15-17]. Nevertheless, three tautomeric forms of free base A, B and C and one anionic D were described for guanfacine in different media by Tomas *et al* [2] but the cationic E and hydrochloride F forms proposed by us in this work were not reported yet. These A, B, C, D, E and F guanfacine structures are presented in **scheme 1**. Note that the hydrochloride form F correspond to the neutral form of cationic E. However, other possible cationic G form was suggested by Tünde Jurca and Florin in the study on interaction of metal ions with guanfacine, as can be seen in **scheme 2** [5]. Hence, other hydrochloride H structure could be also observed as a consequence of cationic G form. In this context, it is very important to identify what hydrochloride structure is the most stable taking into account that it pharmacological drug is the most used form of guanfacine.



**Scheme 1.** Free bases, cationic, anionic and hydrochloride structures of guanfacine in different media.



**Scheme 2.** Additional cationic and hydrochloride structures of guanfacine

Here, it is necessary to remember that the hydrochloride form in aqueous solution is presents as cationic one and, probably due to their higher solubility is quickly adsorbed in the human body [18-25]. Therefore, the aims of this work are the determinations of the most stable free base, cationic, anionic and hydrochloride species of guanfacine in gas phase and in aqueous solution in order to perform the complete vibrational assignments of these species because they are important to their identifications in different media by using the infrared and Raman spectra. So far, the structures and vibrational spectra of all species of guanfacine were not studied. To achieve these purposes the eight structures presented in both schemes were theoretically modeled and optimized in gas phase and in aqueous solution by using DFT calculations and the hybrid B3LYP/6-31G\* method [26,27], in order to predict their vibrational spectra which later were combined with the experimental available infrared and Raman spectra and with the aid of Scaled Mechanical Quantum Force Field (SQMFF) methodology and the Molvib program the complete assignments of all these species were reported [28-30]. Here, all calculations in aqueous solution were performed by using Self-Consistent Reaction Field (SCRF) calculations [31-33]. In addition, the solvation energies, dipole moment values of those structures were compared and analyzed together with their reactivities and behaviors in both media [34-44]. In the same way, the theoretical geometrical parameters for all species were also compared with the corresponding experimental ones determined by X-ray diffraction [2].

### Mechanical quantum calculations

The *GaussView* program [45] was used to model the eight structures of guanfacine while with the Revision A.02 of Gaussian program were carried out the corresponding optimizations in gas phase and in aqueous solution [46]. Here, the Integral Equation F variant Polarised Continuum Method (IEFPCM) was employed in solution while the solvation energies of all species were predicted with the universal solvation model [31-33]. The structure of free base B was experimentally determined by Tomas et al [2] while the cationic E and hydrochloride F

species, proposed by us in this work, can be seen in **Figure 1** and the other tautomeric forms of free base, A and C together with the anionic D form are presented in **Figure 2**. **Figure 3** shows the structures of cationic G form and its corresponding neutral hydrochloride H form.

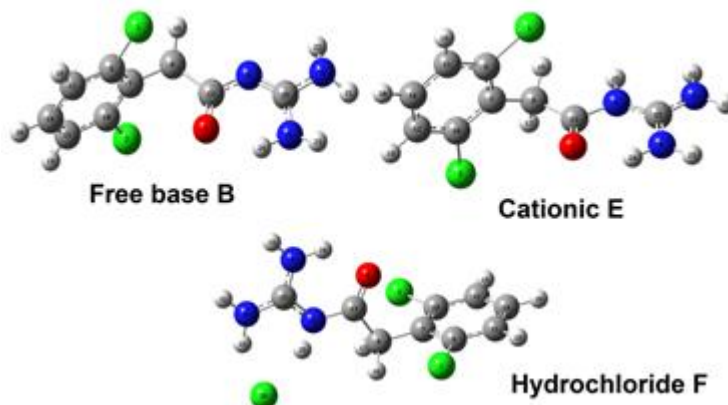


**Figure 1.** Theoretical molecular structures of free base B, cationic E and hydrochloride F species of *N*-(diaminomethylidene)-2-(2,6-dichlorophenyl)acetamide and atoms labeling.

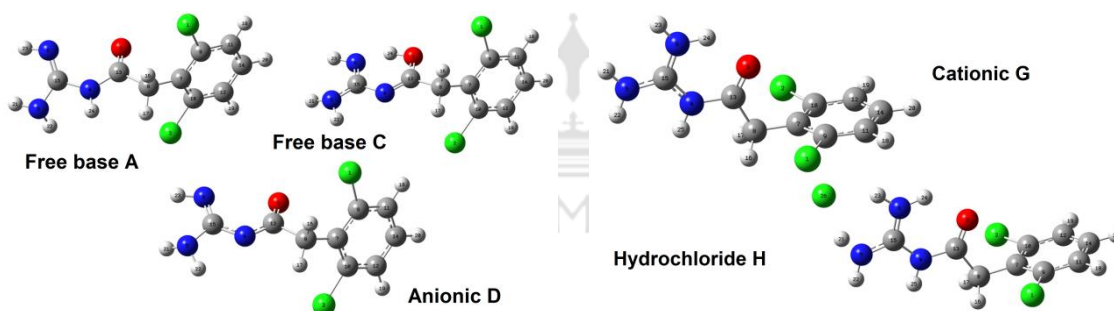


**Figure 2.** Theoretical molecular structures of free bases A and C and anionic species of *N*-(diaminomethylidene)-2-(2,6-dichlorophenyl)acetamide and atoms labeling.

**Figure 3.** Theoretical molecular structures of cationic G and hydrochloride H species of *N*-(diaminomethylidene)-2-(2,6-dichlorophenyl)acetamide and atoms labeling.

Corrections by Zero Point Vibrational Energy (ZPVE) were carried out for the solvation energies of all species while the volumes in both media were computed with the Moldraw program [47]. The reactivities and behaviours of all species were predicted with the frontier orbitals and some interesting descriptors [34-44] while the vibrational analyses were performed with the SQMFF methodology and the Molvib program by using transferable scaling factors and the normal internal coordinates. Hence, for all species, harmonic force fields and force constants were obtained [28-30]. To perform the vibrational assignments of bands observed in the infrared and Raman spectra to the normal vibration modes, only Potential Energy Distribution (PED) contributions major or equal to 10% were considered. Better correlations

in the Raman spectra were observed when the theoretical spectra expressed in activities were converted to intensities [48-49].

## RESULTS AND DISCUSSION

### *Studies of all species in both media*

Calculated total uncorrected and corrected by ZPVE energies, dipole moments and volumes (V) of three tautomeric forms of free base (A, B and C), one anionic (D), two cationic (E and G) and two hydrochloride species (F and H) of guanfacine in gas phase and in aqueous solution are summarized in **Table 1**. All calculations were performed by using the B3LYP/6-31G\* method. In the gas phase, the cationic G and the hydrochloride H species were optimized with imaginary frequencies while in solution only the hydrochloride F species presents imaginary frequencies.

**Table 1. Calculated total energies (E), dipole moments ( $\mu$ ) and volumes (V) of free base, cationic and hydrochloride species of guanfacine in gas phase and in aqueous solution by using the B3LYP/6-31G\* method.**

B3LYP/6-31G* Method				
Gas Phase				
Species	E (Hartrees)	ZPVE (Hartrees)	$\mu$ (D)	V ( $\text{\AA}^3$ )
Free base A	-1508.2469	-1508.0707	4.36	226.3
Free base B	-1508.2720	-1508.0955	3.49	229.6
Free base C	-1508.2550	-1508.0799	2.05	232.5
Anionic D	-1507.6747	-1507.5130	9.69	228.4
Cationic E	-1508.6567	-1508.4676	13.98	231.4
Cationic G <sup>#</sup>	-1508.6566	-1508.4676	14.31	231.8
Hydrochloride F	-1969.1013	-1968.9130	8.89	251.9
Hydrochloride H <sup>#</sup>	-1969.0907	-1968.9024	13.49	252.5
Aqueous Solution				
Free base A	-1508.2800	-1508.1033	7.59	227.3
Free base B	-1508.2956	-1508.1202	5.43	229.8
Free base C	-1508.2956	-1508.1202	5.43	229.3
Anionic D	-1507.7858	-1507.6229	12.10	229.1
Cationic E	-1508.7601	-1508.5708	17.53	230.8
Cationic G <sup>#</sup>	-1508.7601	-1508.5708	17.53	231.2
Hydrochloride F <sup>#</sup>	-1969.1402	-1968.9512	12.26	253.1
Hydrochloride H	-1969.1381	-1968.9487	17.69	252.7

<sup>#</sup>Imaginary frequencies

The results of Table 1 show that the tautomeric free base B form is the only most stable free base in gas phase than the other ones and it presents the higher volume in this medium while in solution, the free base forms B and C show the same energy values and both species are the

most stable increasing its dipole moments values in this medium. In solution, both cationic forms E and G show the same energy and dipole moment values but both forms evidence different volumes in the two media. From both hydrochloride forms, the F form is the most stable in gas phase but in solution the F form presents imaginary frequency while the form H in gas phase was optimized with imaginary frequency. In **Figure 4** it is presented the variations in the dipole moment values and volumes for all species in both media.

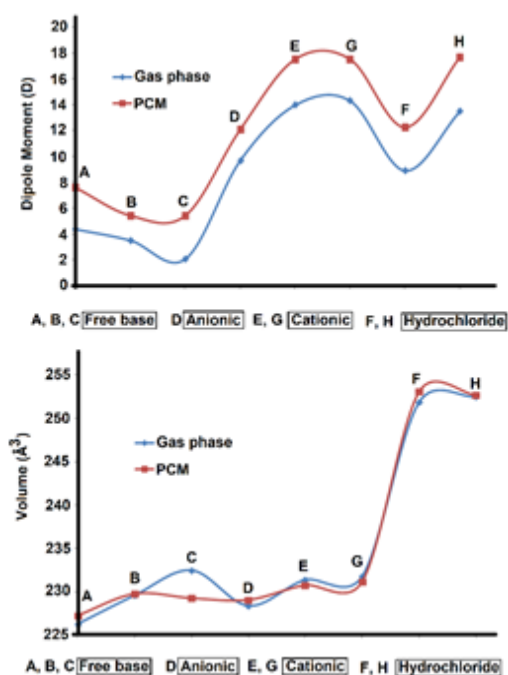


**Figure 4. Behaviours of dipole moments (upper) and volumes (bottom) corresponding to the eight species of guanfacine in both media.**

From **Figure 4** can be easily seen that the two cationic forms E and G together with the hydrochloride form H present the higher dipole moment values in both media while the free base C in gas phase has the lowest value. Obviously, the cationic charged species increase the dipole moment values in solution. Note that in solution, all species increase the dipole moment values due to their respective hydrations with solvent molecules.

In relation to the volumes, practically the same behaviours are observed for all species in both media with exception of value for free base C where it is observed a significant diminishing in solution.

Obviously, the hydrochloride species present the higher volumes in both media due to voluminous size of Cl atom. From Table 1, we observed that the total energy values corrected by ZPVE in both media present lower values than those uncorrected, a resulted similar to those observed in the free base, cationic and hydrochloride species of 2C-B, gramine and eucalyptol [25,50,51]. Corrected and uncorrected solvation energies by the total non-electrostatic terms and by ZPVE of eight species of guanfacine by using the B3LYP/6-31G\* method are presented in **Table 2** while in **Table 3** are presented comparisons of most stable free base, cationic and hydrochloride species of guanfacine with the values determined for scopolamine, morphine,

heroin, cocaine and tropane alkaloids [18-22], cyclizine, gramine [24,50] and 2C-B [25]. On the other hand, the behaviours of corrected solvation energies and volume variations of eight different species of guanfacine can be easily seen in **Figure 5** while comparisons and behaviours of corrected solvation energies of most stable free base, cationic and hydrochloride species of guanfacine with the values reported for other species are given in **Figure 6**.

**Table 2. Corrected and uncorrected solvation energies by the total non-electrostatic terms and by zero point vibrational energy (ZPVE) of free base, cationic, anionic and hydrochloride species of guanfacine in aqueous solution by using the B3LYP/6-31G\* method.**

B3LYP/6-31G* method <sup>a</sup>				
Species	Solvation energy (kJ/mol)			$\Delta V$ (Å <sup>3</sup> )
	$\Delta G_{un}^{\#}$	$\Delta G_{ne}$	$\Delta G_c$	
Free base A	-85.51	20.10	-105.61	1.0
Free base B	-64.79	16.80	-81.59	0.2
Free base C	-105.71	16.80	-122.51	-3.2
Anionic D	-288.27	13.33	-301.60	0.7
Cationic E	-270.69	23.20	-293.89	-0.6
Cationic G <sup>#</sup>	-270.69	23.20	-293.89	-0.6
Hydrochloride F	-100.20	22.40	-122.60	1.2
Hydrochloride H	-121.44	22.15	-143.59	0.2

<sup>a</sup>This work

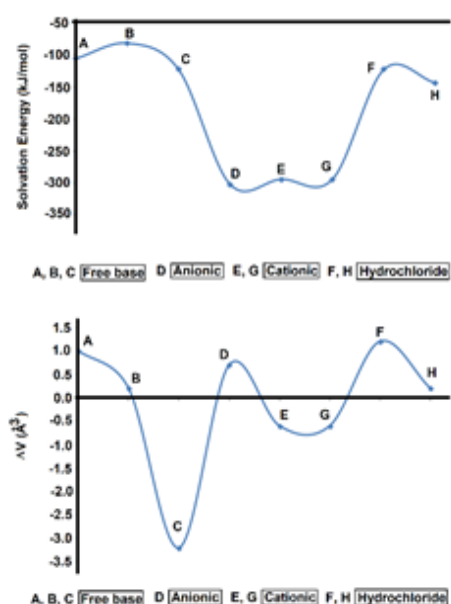
$\Delta G_{un}^{\#}$ = uncorrected solvation energy,  $\Delta G_{ne}$ = total non-electrostatic terms,  $\Delta G_c$ = corrected solvation energies. <sup>a</sup>This work.

**Table 3. Corrected and uncorrected solvation energies by the total non-electrostatic terms and by zero point vibrational energy (ZPVE) of free base, cationic and hydrochloride species of guanfacine in aqueous solution by using the B3LYP/6-31G\* method.**

B3LYP/6-31G* method <sup>a</sup>			
Species	$\Delta G_c$ , Solvation energy (kJ/mol)		
	Free base	Cationic	Hydrochloride
Guanfacine <sup>a</sup>	-81.59	-293.89	-143.59
Gramine <sup>b</sup>	-34.89	-261.58	-115.51
2C-B <sup>c</sup>	-49.31	-308.69	-122.58
S(-)-Promethazine <sup>d</sup>	-36.07	-14.48	-70.44
R(+)-Promethazine <sup>d</sup>	-17.87	-262.81	-52.02
Cyclizine <sup>e</sup>	-29.53	-244.36	-105.06
Morphine <sup>f</sup>	-60.91	-309.19	-144.74
Cocaine <sup>g</sup>	-71.26	-255.24	-138.14
Scopolamine <sup>h</sup>	-75.47	-310.34	-122.74
Heroin <sup>i</sup>	-88.67	-323.14	-161.94
Tropane <sup>j</sup>	-12.55	-244.33	-87.18

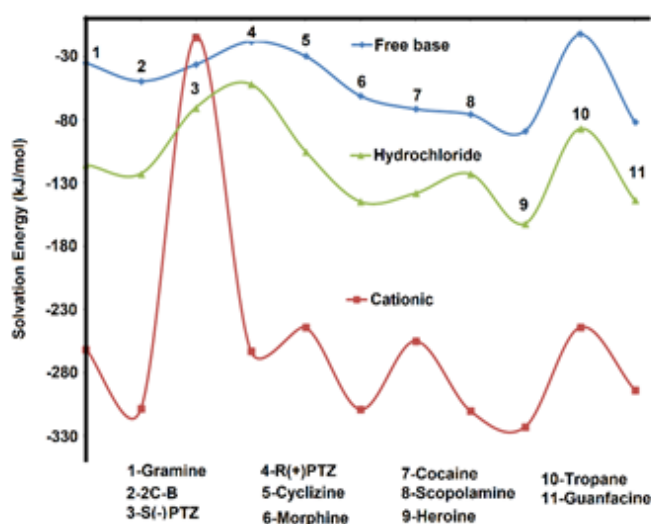
<sup>a</sup>This work, <sup>b</sup>From Ref [50], <sup>c</sup>From Ref [25], <sup>d</sup>From Ref [52], <sup>e</sup>From Ref [24], <sup>f</sup>From Ref [18],  
<sup>g</sup>From Ref [20], <sup>h</sup>From Ref [43], <sup>i</sup>From Ref [21], <sup>j</sup>From Ref [19]

Table 2 and Figure 5 show that the charged D, E and G species present higher solvation energies, as expected, because these species are most hydrated in solution due to their charges and, in particular, the anionic D species presents the highest value. Later, the two cationic E and G species have the same values indicating probably that the solvation energy values for these species are independent on the position of positive charges on the N atoms, those are, on the N-H group in the cationic form E or on NH<sub>2</sub> group in the cationic form G, as observed from Scheme 2.



**Figure 5. Comparisons of corrected solvation energies (upper) and volume variations (bottom) of free base, cationic and hydrochloride species of guanfacine with those corresponding to other species by using the B3LYP/6-31G\* method.**

Moreover, the free base B has the lowest corrected solvation energy in aqueous solution (-81.59 kJ/mol) and the lower volume variation (0.2 Å<sup>3</sup>) together with the hydrochloride form H. In relation to the volume variations, Figure 5 shows clearly that the two cationic E and G species (-0.6 Å<sup>3</sup>) and the free base C present volume contractions, being most notable in the free base C with a value of -3.2 Å<sup>3</sup> while volume expansions are observed in the other species. The hydrochloride form F together with the free base A present the higher volume expansions in solution (1.2-1.0 Å<sup>3</sup>).



In Figure 6 are observed the different behaviors for the free base B, cationic G and hydrochloride H species of guanfacine with the corresponding to gramine [50], 2C-B [25], S(-)- and R(+)-Promethazine [52], cyclizine [24], morphine [18], cocaine [20], scopolamine [43], heroin [21] and tropane [19].

**Figure 6. Comparisons of corrected solvation energies of free base, cationic and hydrochloride species of guanfacine with those corresponding to other species by using the B3LYP/6-31G\* method.**

Here, it is necessary to clarify that the compared species of guanfacine presented in Table 2 are the free base B because it species is the most stable than the other ones (see Table 1) and the cationic form G and the hydrochloride form H because both species were optimized with all positive frequencies. Figure 6 shows that free base species of all compounds present the lower corrected solvation energies values, presenting the species corresponding to tropane the lowest value. Note that all cationic species have higher corrected solvation energies values where clearly the species of 2C-B and heroin have the highest values. Here, from Table 3 and Figure 6 we observed that the free base B of guanfacine (-81.59 kJ/mol) present a next value to heroin (-88.67 kJ/mol), the cationic form G (-293.89 kJ/mol) has a value near to 2C-B (-308.69 kJ/mol) and, finally, the solvation energy value for the hydrochloride form H of guanfacine (-143.59 kJ/mol) is closer to value of morphine (-144.74 kJ/mol).

### ***Geometries of all species in both media***

Calculated geometrical parameters for the six species of guanfacine in gas phase by using the hybrid B3LYP/6-31G\* method are compared in **Table 4** with those experimental determined by Tomas et al [2] for the free base B by using the root-mean-square deviation (RMSD) values. In **Table 5** are presented the values in solution.

**Table 4. Comparisons of calculated geometrical parameters of six species of guanfacine in gas phase with experimental values taken for free base from Ref [2].**

B3LYP/6-31G* Method							
Parameters	Free base		Anionic	Cationic	Hydrochloride	Experimental <sup>b</sup>	
	A	B	C	D	E		F
Bond lengths (Å)							
C7-C8	1.505	1.505	1.511	1.508	1.508	1.505	1.494(3)
C8-C13	1.542	1.534	1.517	1.516	1.516	1.523	1.526(3)
C13-O3	1.210	1.237	1.313	1.211	1.211	1.224	1.241(3)
N4-C13	1.389	1.373	1.303	1.427	1.427	1.387	1.342(3)
N4-C15	1.413	1.320	1.390	1.366	1.366	1.364	1.351(3)
N5-C15	1.272	1.372	1.372	1.337	1.337	1.325	1.325(3)
N6-C15	1.403	1.353	1.303	1.322	1.322	1.335	1.323(3)
<b>RMSD<sup>b</sup></b>	<b>0.049</b>	<b>0.027</b>	<b>0.040</b>	<b>0.035</b>	<b>0.035</b>	<b>0.020</b>	
Bond angles (°)							
C7-C8-C13	112.3	113.8	114.5	112.7	112.7	113.0	113.0(2)
O3-C13-C8	122.8	120.6	115.1	125.4	125.4	124.1	118.1(2)
N4-C13-C8	112.3	111.6	118.1	120.7	113.7	112.5	113.9(2)
O3-C13-N4	124.8	127.6	126.6	120.7	120.7	123.3	128.0(2)
C13-N4-C15	127.0	119.4	118.0	125.8	125.8	125.8	120.2(2)
N4-C15-N5	121.1	116.9	112.3	118.3	118.3	116.4	116.7(2)
N4-C15-N6	109.9	126.1	122.5	120.0	120.0	120.2	125.0(2)
N5-C15-N6	128.7	116.8	125.1	121.5	121.5	123.2	118.3(2)
<b>RMSD<sup>b</sup></b>	<b>7.4</b>	<b>1.4</b>	<b>3.7</b>	<b>5.3</b>	<b>4.7</b>	<b>4.2</b>	
Dihedral angles (°)							
C7-C8-C13-N4	154,4	179,3	147,8	-153,3	-153,3	179,9	
C8-C13-N4-C15	170,0	176,9	177,2	-177,7	-177,7	179,9	
C13-N4-C15-N5	-35,4	-173,6	-177,4	-179,7	-179,7	0,0	
C13-N4-C15-N6	149,0	5,9	0,8	0,31	0,3	-179,9	

<sup>a</sup>This work, <sup>b</sup>Ref [2], Cation G and hydrochloride H present imaginary frequencies

**Table 5. Comparisons of calculated geometrical parameters of derived species from guanfacine in aqueous solution with experimental values taken for free base from [2].**

B3LYP/6-31G* Method						
Parameters	Free base		Anionic	Cationic	Hydrochloride	Experimental <sup>b</sup>
	A	B=C	D	E=G	H	
Bond lengths (Å)						
C7-C8	1.505	1.506	1.506	1.506	1.506	1.494(3)
C8-C13	1.534	1.534	1.550	1.519	1.521	1.526(3)
C13-O3	1.226	1.252	1.263	1.223	1.224	1.241(3)
N4-C13	1.373	1.354	1.329	1.391	1.388	1.342(3)
N4-C15	1.411	1.344	1.384	1.374	1.377	1.351(3)
N5-C15	1.386	1.352	1.405	1.326	1.326	1.325(3)
N6-C15	1.282	1.340	1.301	1.320	1.321	1.323(3)
<b>RMSD<sup>b</sup></b>	<b>0.038</b>	<b>0.015</b>	<b>0.037</b>	<b>0.022</b>	<b>0.022</b>	
Bond angles (°)						
C7-C8-C13	112.9	113.9	113.5	112.8	112.8	113,0(2)
O3-C13-C8	122.6	119.2	117.4	123.8	124.0	118,1(2)
N4-C13-C8	112.2	128.1	112.8	113.4	113.1	113,9(2)
O3-C13-N4	125.0	128.1	129.7	122.6	122.8	128,0(2)
C13-N4-C15	129.1	120.1	121.4	126.6	126.8	120,2(2)
N4-C15-N5	110.8	116.6	111.7	117.4	118.0	116,7(2)
N4-C15-N6	121.8	125.6	125.3	120.6	121.1	125,0(2)
N5-C15-N6	127.1	117.7	122.4	121.8	120.7	118,3(2)
<b>RMSD<sup>b</sup></b>	<b>5.4</b>	<b>5.1</b>	<b>2.5</b>	<b>4.1</b>	<b>4.0</b>	
Dihedral angles (°)						
C7-C8-C13-N4	-173.2	168.7	152.5	-164.7	-177.9	
C8-C13-N4-C15	-176.8	178.7	170.2	-177.9	-178.5	
C13-N4-C15-N5	166.9	-176.5	144.8	-177.3	179.3	
C13-N4-C15-N6	-17.2	2.2	-42.8	2.8	-0.5	

<sup>a</sup>This work, <sup>b</sup>Ref [2], Hydrochloride F imaginary frequencies

Table 4 shows that the better correlations in bond lengths in gas phase are observed for the free base B and the hydrochloride F species (0.027-0.020 Å) while the lower RMSD value for bond angles only for the free base B is observed. In solution, the RMSD values decrease presenting the lowest value in bond lengths the free base B. Analyzing the bond lengths, the C13=O3 distance for the free base C presents the lower value but in solution the double bond character decreases while the N4-C15 distances for the free base in both media present the lower values confirming the double bond character only for this species, as observed in Scheme 1 and Fig. 1. Note that the N4-C13 bond present double bond character in the free base C in gas phase

and in the anionic D species in solution, as expected because this anion exist only in this media. In relation to N5-C15 bond, the free base A present the higher value in gas phase while in the other species this bond present partial double bond character. In the free base A in gas phase, the N6-C15 distance practically has simple bond character while in all species have double bond character in solution. On the other hand, the differences among the species in gas phase and in aqueous solution can be easily seen from dihedral angles. Thus, in **Figure 7** are presented the most important changes only observed for the dihedral angles of the free base A and anionic D species of guanfacine in both media.

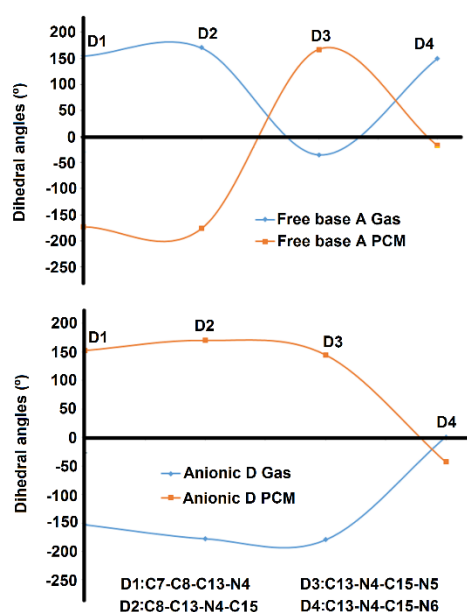


**Figure 7. Variations in dihedral angles for the free base A and anionic D species of guanfacine in both media by using the B3LYP/6-31G\* method.**

The four dihedral angles considered are D1: C7-C8-C13-N4, D2: C8-C13-N4-C15, D3: C13-N4-C15-N5 and D4: C13-N4-C15-N6. The tautomeric free base A presents the four dihedral angles in gas phase different from the values observed in aqueous solution while in the anionic D species the dihedral D1, D2 and D3 present approximately the same values and negative signs in gas phase changing to positive signs in solution. On the contrary, the dihedral angles D4 in both media have different signs than the other ones, as can be seen in Fig. 7.

The low RMSD values in the bond lengths and angles of all species of guanfacine suggest that these structures can be used to perform the vibrational assignments.

### *Frontier orbitals and quantum global descriptors studies*

The gap values for all species of guanfacine in both media were calculated according Parr and Pearson by using the frontier orbitals [53]. From the differences between both orbitals for each

species were computed the chemical potential ( $\mu$ ), electronegativity ( $\chi$ ), global hardness ( $\eta$ ), global softness ( $S$ ), global electrophilicity index ( $\omega$ ) and global nucleophilicity index (E) descriptors by means of characteristics equations and the hybrid B3LYP/6-31G\* level of theory [34-44]. Thus in **Table 6** are presented the gap values together with the descriptors for all species of guanfacine in both media.

**Table 6. Frontier molecular orbitals, gap values and descriptors for all species of guanfacine in gas phase and in aqueous solution by using the B3LYP/6-31G\* level of theory.**

GAS PHASE						
Orbital	Free base			Anionic	cation	hydrochloride
	A	B	C	D	E	F
HOMO	-6.5983	-6.4683	-6.7021	-0.9308	-9.4806	-5.8096
LUMO	-0.6566	-0.3734	-0.6092	2.4918	-5.3392	-1.4160
GAP	5.9417	6.0949	6.0929	3.4226	4.1414	4.3936
Descriptors						
Descriptor	A	B	C	D	E	F
$\chi$	-2.9709	-3.0475	-3.0465	-1.7113	-2.0707	-2.1968
$\mu$	-3.6275	-3.4209	-3.6557	0.7805	-7.4099	-3.6128
$\eta$	2.9709	3.0475	3.0465	1.7113	2.0707	2.1968
$s$	0.1683	0.1641	0.1641	0.2922	0.2415	0.2276
$\omega$	2.2146	1.9200	2.1933	0.1780	13.2580	2.9708
E	-10.7766	-10.4249	-11.1368	1.3357	-15.3437	-7.9366
AQUEOUS SOLUTION						
Orbital	Free base		Anionic	cation	hydrochloride	
	A	B=C	D	E=G	H	
HOMO	-6.4803	-6.2843	-0.6700	-9.3846	-4.9437	
LUMO	-0.6452	-0.2563	2.4584	-5.4117	-1.8675	
GAP	5.8351	6.0280	3.1284	3.9729	3.0762	
Descriptors						
Descriptor	A	B=C	D	E=G	H	
$\chi$	-2.9176	-3.0140	-1.5642	-1.9865	-1.5381	
$\mu$	-3.5628	-3.2703	0.8942	-7.3982	-3.4056	
$\eta$	2.9176	3.0140	1.5642	1.9865	1.5381	
$s$	0.1714	0.1659	0.3197	0.2517	0.3251	
$\omega$	2.1753	1.7742	0.2556	13.7765	3.7703	
E	-10.3945	-9.8567	1.3987	-14.6961	-5.2382	

<sup>a</sup>This work

$$\chi = - [E(\text{LUMO}) - E(\text{HOMO})]/2 ; \mu = [E(\text{LUMO}) + E(\text{HOMO})]/2 ; \eta = [E(\text{LUMO}) - E(\text{HOMO})]/2;$$

$$S = 1/2\eta ; \omega = \mu^2/2\eta \quad E = \mu * \eta$$

In gas phase, the anionic D species has the low gap value and, for this reason, it species is the most reactive while in solution the hydrochloride H species is the most reactive together with the anionic species. Here, the three tautomeric free bases are the less reactive species in both media, being in particular the B species the less reactive. For these reasons, from pharmacological point of view the hydrochloride species are the preferred for the preparations and design of new drugs. Evaluating the descriptors, we observed that in solution the value decrease, as compared with the values in gas phase. Both cationic species E and G show high global nucleophilicity (E) and electrophilicity indexes ( $\omega$ ) values while, on the contrary, the anionic D species in both media show the lower values of both indexes.

### ***Vibrational study***

The structures corresponding to the anionic D, three free bases A, B and C, the two cationic E and G and the two hydrochloride F and H species of guanfacine in both media were optimized with  $C_1$  symmetries. The expected normal vibration modes for the anionic, free bases, cationic and hydrochloride species are 63, 66, 69 and 72, respectively. In **Figure 8** are compared the experimental available infrared spectrum of free base species of guanfacine in the solid state with the corresponding predicted for the three free bases A, B and C and for the anionic D by using the hybrid B3LYP/6-31G\* method while in **Figure 9** are compared the experimental IR spectrum with the predicted for the two cationic and hydrochloride species. Both experimental available infrared and Raman spectrum were taken from [4,8]. In **Figure 10** are compared the experimental available Raman spectrum of free base of guanfacine with the corresponding predicted for the three free bases A, B and C and for the anionic D species while in **Figure 11** the experimental Raman spectrum are compared with the predicted for the two cationic E, G and for the hydrochloride F and H species by using the hybrid B3LYP/6-31G\* method. Here it is necessary to clarify that all theoretical IR and Raman spectra presented in the Figures from 8 to 11 correspond to predicted for all species in gas phase with exception of spectra presented in Figures 9 and 11 which correspond to the cationic G and hydrochloride H species in aqueous solution because they were optimized in gas phase with imaginary frequencies, as observed in Table 1. The Raman spectra for all species predicted in activities were transformed to intensities by means of recognised equations proposed [48,49]. From Fig. 8 we can easily see that the better IR spectra correlations are observed for the free base B although the band of medium intensity at  $775\text{ cm}^{-1}$  is only justified by the cationic E species. However, the anionic

D species also shows a band in this region but this species only exists when the enol OH group in the tautomeric form C is deprotonated in alkaline medium [2].

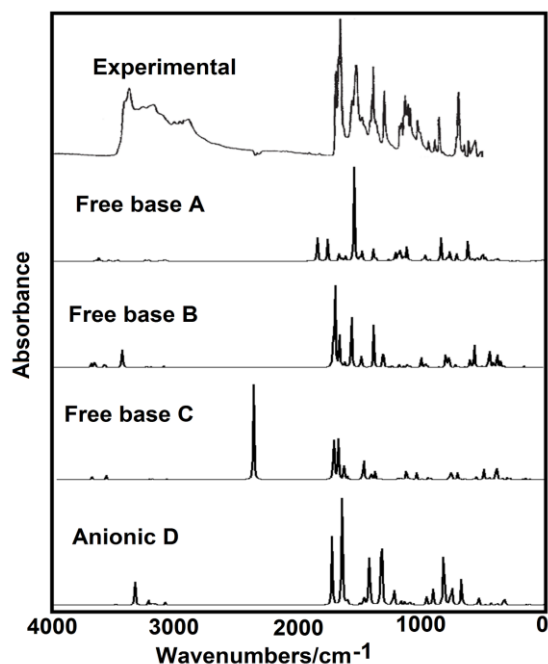


**Figure 8. Experimental available infrared spectrum of free base species of guanfacine in solid phase [4] compared with the predicted for free bases and anionic species by using the hybrid B3LYP/6-31G\* method.**

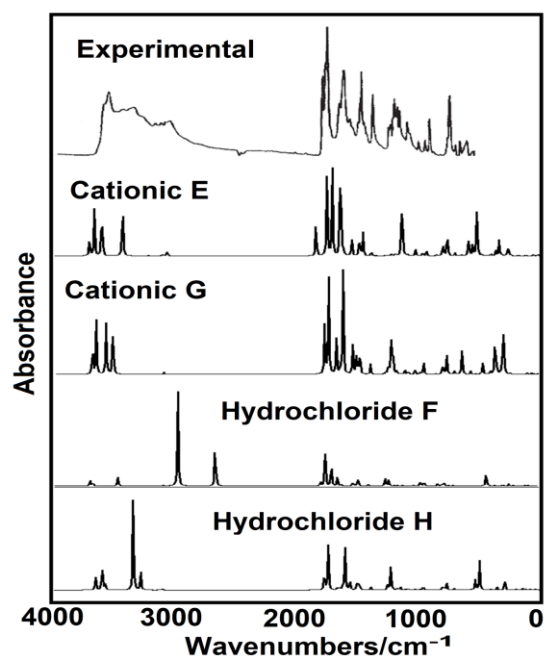


**Figure 9. Experimental available infrared spectrum of free base species of guanfacine in solid phase [4] compared with the predicted for cationic and hydrochloride species by using the hybrid B3LYP/6-31G\* method.**

From experimental IR spectrum, it is easy to see that the hydrochloride F and H forms are not present in the solid phase because the very strong IR bands predicted at  $2549\text{ cm}^{-1}$  in the form E and at  $3329\text{ cm}^{-1}$  in the form H are not observed in the experimental spectrum. Hence, these results are similar to those observed in some alkaloids and antihistaminic hydrochloride species where the hydrochloride forms are not present in the solid phase [18-25]. The harmonic force fields for all species of guanfacine were computed at the same level of theory by using their corresponding normal internal coordinates with the SQMFF approach [28] and the Molvib program [30]. In the scaling, process were employed the scale factors suggested by Rauhut and Pulay [29]. The scaled force fields and PED contributions higher or equal to 10% were used to perform the complete vibrational assignments of all normal vibration modes to the bands observed in both infrared and Raman spectra. The observed and calculated wavenumbers and

assignments for the most stable free base B, the cationic E, hydrochloride F and anionic D species of guanfacine are summarized in **Table 7**. Then, a brief discussion of some vibration modes are presented at continuation.

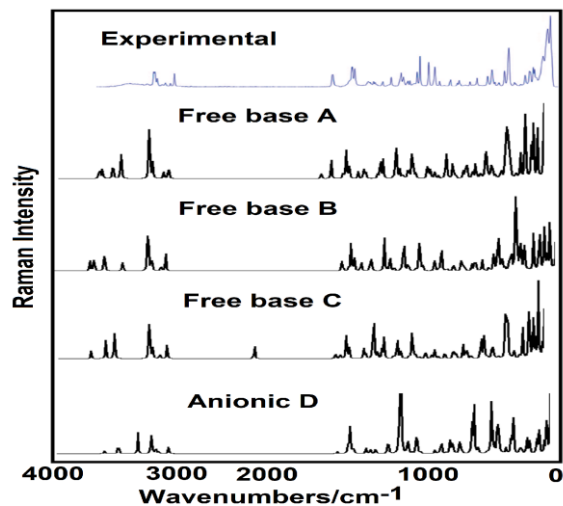


**Figure 10.** Experimental available infrared spectrum of free base species of guanfacine in solid phase [8] compared with the predicted for free bases and anionic species by using the hybrid B3LYP/6-31G\* method.

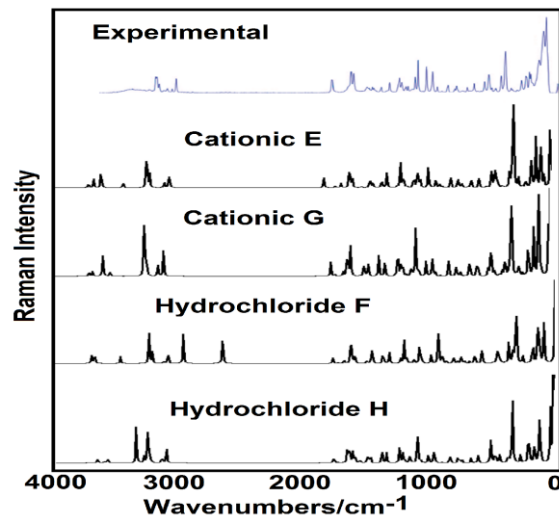


**Figure 11.** Experimental available infrared spectrum of free base species of guanfacine in solid phase [8] compared with the predicted for cationic and hydrochloride species by using the hybrid B3LYP/6-31G\* method.

**Table 7. Observed and calculated wavenumbers (cm<sup>-1</sup>) and assignments of most stable free base, anionic, cationic and hydrochloride species of guanfacine.**

Experimental		B3LYP/6-31G* Method <sup>a</sup>								
		Free base B		Cationic E		Hydrochloride F		Anionic D		
IR <sup>c</sup>	Raman <sup>d</sup>	SQM <sup>b</sup>	Assignments <sup>a</sup>	SQM <sup>b</sup>	Assignments <sup>a</sup>	SQM <sup>b</sup>	Assignments <sup>a</sup>	SQM <sup>b</sup>	Assignments <sup>a</sup>	
		3534	v <sub>a</sub> NH <sub>2</sub> (N5)	3546	v <sub>a</sub> NH <sub>2</sub> (N5)	3534	v <sub>a</sub> NH <sub>2</sub> (N6)			
		3503	v <sub>a</sub> NH <sub>2</sub> (N6)	3507	v <sub>a</sub> NH <sub>2</sub> (N6)					
3350m		3425	v <sub>s</sub> NH <sub>2</sub> (N5)	3454	vN4-H25	3511	v <sub>a</sub> NH <sub>2</sub> (N5)	3442	v <sub>a</sub> NH <sub>2</sub> (N5)	
3329s	3317w			3444	v <sub>s</sub> NH <sub>2</sub> (N5)	3315	v <sub>s</sub> NH <sub>2</sub> (N6)	3338	v <sub>s</sub> NH <sub>2</sub> (N5)	
3210m	3283w	3288	v <sub>s</sub> NH <sub>2</sub> (N6)	3286	v <sub>s</sub> NH <sub>2</sub> (N6)			3188	vN6-H23	
3150m	3147w	3099	vC12-H19	3107	vC12-H19	3101	vC11-H18	3087	vC11-H18	
		3096w	3095	vC11-H18	3104	vC11-H18	3098	vC12-H19	3082	vC12-H19
3000m	3074m	3070	vC14-H20			3074	vC14-H20	3053	vC14-H20	
2900m	3031w	3001	v <sub>a</sub> CH <sub>2</sub> (C8)	3084	vC14-H20	2993	v <sub>a</sub> CH <sub>2</sub> (C8)	3029	v <sub>a</sub> CH <sub>2</sub> (C8)	
2973w	3004w			2974	v <sub>a</sub> CH <sub>2</sub> (C8)	2957	v <sub>s</sub> CH <sub>2</sub> (C8)			
2858w	2917m	2964	v <sub>s</sub> CH <sub>2</sub> (C8)	2934	v <sub>s</sub> CH <sub>2</sub> (C8)	2842	v <sub>s</sub> NH <sub>2</sub> (N5)	2954	v <sub>s</sub> CH <sub>2</sub> (C8)	
						2549	vN4-H25			
1700m	1751m			1772	vC13=O3	1724	vC13=O3			
1690s		1648	vC13=O3	1687	vC15-N6 vC15-N5	1695	ρN4-H25 vC15-N5	1668	vC13=O3	
1690s		1633	vN4-C15	1634	δNH <sub>2</sub> (N5)	1633	δNH <sub>2</sub> (N5)	1594	vC15-N6 δN5C15N4 δN6C15N5	
	1584m	1594	δNH <sub>2</sub> (N5) vC15-N6	1583	vC9-C11	1588	ρN4-H25	1580	vC9-C11	
1570m	1565m	1586	vC9-C11 vC10-C12	1579	δNH <sub>2</sub> (N5) vN4-C15	1586	vC10-C12 vC9-C11	1575	δNH <sub>2</sub>	
1510w		1562	vC14-C12 vC14-C11	1563	vC14-C11 vC14-C12	1563	vC14-C12 vC14-C11	1555	vC14-C12 vC14-C11	
1450m	1458w	1507	vC15-N5	1486	δNH <sub>2</sub> (N6)	1462	δNH <sub>2</sub> (N6)			
	1438w	1437	βC12-H19 vC7-C10	1441	βC12-H19 vC7-C10	1439	βC11-H18 vC7-C9	1443	δCH <sub>2</sub>	
		1435	βC11-H18	1435	βC11-H18 vC7-C9	1437	βC14-H20 βC12-H19	1430	βC11-H18	
		1427	δNH <sub>2</sub> (N6)					1424	vC7-C10	
	1414w	1423	δCH <sub>2</sub>	1413	ρN4-H25	1429	ρN4-H25 δN4H25C126	1390	δN6C15N4 δN6C15N5	
1410s	1401w			1403	δCH <sub>2</sub>	1417	δCH <sub>2</sub>			
1350m	1344w	1348	wagCH <sub>2</sub> vC8-C13 vN4-C13	1363	wagCH <sub>2</sub>	1367	wagCH <sub>2</sub>			
	1288w	1291	vC7-C9 vC7-C10	1300	ρCH <sub>2</sub> vC7-C10	1298	vC7-C10	1293	vN4-C13 vN4-C15	
	1288w	1272	wagCH <sub>2</sub> vN4-C13					1284	vC7-C9	
	1212w			1228	ρCH <sub>2</sub> vC10-C12	1226	ρCH <sub>2</sub> vC9-C11 vC10-C12	1221	wagCH <sub>2</sub> vC8-C13	
	1202m	1219	ρCH <sub>2</sub> vC9-C11			1213	vN4-C13	1214	vC10-C12 βC12-H19	
1182sh	1174w	1193	vC7-C8	1198	vC7-C8	1192	vC7-C8	1187	vC7-C8	
1170s				1181	βC12-H19	1175	βC12-H19			
1155m	1155w	1165	βC14-H20 βC12-H19					1151	βC14-H20	
1128m	1135w	1136	ρCH <sub>2</sub>	1151	βC14-H20	1145	βC14-H20	1145	ρNH <sub>2</sub> δH23N6C15	
1095m	1102w			1100	ρC13=O3					
	1095s	1105	ρNH <sub>2</sub> (N6)	1096	ρNH <sub>2</sub> (N6)	1117	ρNH <sub>2</sub> (N5) vC15-N6	1110	ρCH <sub>2</sub>	
	1071s	1078	ρNH <sub>2</sub> (N5)			1081	ρNH <sub>2</sub> (N6)			

1056m	1068	vC14-C12 vC14-C11	1068	$\beta R_1(A1)$	1070	$\beta R_1(A1)$	1068	$\delta N6C15N4$	
1056m	1066	$\beta R_1(A1)$	1066	vC14-C11 vC14-C12	1068	vC14-C12 vC14-C11	1068	vC14-C12 vC14-C11	
1041sh			1058	$\rho NH_2(N5)$			1058	$\beta R_1(A1)$	
	1005m		998	$\gamma C14-H20$	985	vN4-C15 vC8-C13			
972w	961	$\gamma C14-H20$ vC15-N5	984	vN4-C15 vC8-C13	980	$\gamma C14-H20$			
972w	960	$\gamma C14-H20$							
	950m		934	vN4-C13	944	$\delta C13N4C15$	932	$\gamma C14-H20$	
935m	921	$\delta C13N4C15$					918	$\delta N6C15N4$ $\delta N5C15N4$	
	909w	896	$\tau wCH_2\gamma C13=O3$	916	$\gamma C11-H18$	904	$\gamma C12-H19$ $\gamma C11-H18$	901	$\delta N5C15N4$ $\delta N6C15N4$
888m	889	$\gamma C12-H19$ $\gamma C11-H18$			887	$\tau wCH_2$	877	$\tau wCH_2$ $\gamma C13=O3$	
860w	875w		877	$\tau wCH_2$	863	$\gamma N4-H25$	873	$\gamma C12-H19$ $\gamma C11-H18$	
	842w	836	vC7-C8 $\beta R_1(A1)$	834	vC7-C8 $\delta C7C8C13$	836	vC7-C8 $\delta C7C8C13$	829	$\delta N5C15N4$ $\delta N6C15N5$
807vw			795	$\gamma C12-H19$	788	$\tau R_1(A1)$ $\gamma C11-H18$	811	vC15-N5	
775m	774w	781	$\tau R_1(A1)$	781	$\beta R_3(A1)$ $\rho C13=O3$	776	$\gamma C14-H20$ $\gamma C7-C8$		
775m	774w	771	$\gamma C14-H20$ $\gamma C11-H18$			771	$\tau wNH_2(N5)$	769	$\tau R_1(A1)$ $\delta N5C15N4$
	761w	762	$\gamma C15-N5$					755	$\gamma C14-H20$ $\gamma C12-H19$
									$\beta R_2(A1)$
740w	746	$\beta R_2(A1)$ vC9-C11 vC10-C12	747	vC9-C11	749	$\beta R_2(A1)$	741	vC9-C11v C10-C12 $\beta R_3(A1)$	
	713w		717	$\gamma C15-N5$	723	$\gamma C15-N5$			
	713w		701	$\tau wNH_2(N6)$			702	$\tau N6-C15$	
690w	681	$\tau R_1(A1)$ $\tau wNH_2(N6)$	682	$\tau R_1(A1)$					
	678w	672	$\tau R_1(A1)$		678	$\tau R_1(A1)$	669	wagNH <sub>2</sub>	
650w	657w				644	$\tau wNH_2(N6)$	653	$\tau R_1(A1)$	
627sh	638w	630	$\beta R_3(A1)$	631	$\beta R_3(A1)$	630	$\beta R_3(A1)$	629	$\delta N6C15N5$ $\delta N6C15N4$
600w	570	$\gamma C13=O3$ wagNH <sub>2</sub> (N5)	573	$\gamma N4-H25$					
550w	550m	546	wagNH <sub>2</sub> (N5)	541	$\gamma C13=O3$	543	$\gamma C13=O3$	556	$\delta N6C15N4$ $\delta N6C15N5$
		528	$\gamma C9-C11$ $\gamma C10-C12$	530	$\gamma C9-C11$ $\gamma C10-C12$	533	$\gamma C10-C12$ $\gamma C9-C11$	537	$\delta N6C15N5$ $\delta N6C15N4$
	512w	516	$\tau R_2(A1)$ $\tau R_3(A1)$	520	$\delta N6C15N5$	523	$\delta N6C15N5$	523	$\gamma C9-C11$ $\gamma C10-C12$
	490w		497	$\tau R_2(A1)$					
490w	493	$\delta N6C15N5$	491	wagNH <sub>2</sub> (N6)	504	$\tau R_2(A1)$	489	$\delta N6C15N5$ $\delta N5C15N4$	
		468	$\beta C7-C8$ $\tau wCH_2$	464	$\tau wCH_2$ $\beta C7-C8$	463	$\tau wCH_2$ $\beta C7-C8$	476	$\beta C7-C8$
456w	447	$\rho C15-N4$ $\rho C13=O3$			448	$\rho C15-N4$ $\rho C13=O3$	440	$\delta C13N4C15$ $\delta N5C15N4$ $\delta N6C15N4$	
413m	413	wagNH <sub>2</sub> (N6)	422	$\rho C15-N4$					
403vs	396	$\beta C10-C12$ $\beta C9-C11$			405	$\tau wNH_2(N5)$ wagNH <sub>2</sub> (N5)			
403vs	391	$\tau wNH_2(N5)$	395	$\beta C9-C11$ vC9-C11	396	$\beta C10-C12$ $\beta C9-C11$	398	$\delta C8C13N4\beta$ C10-C12 $\beta C9-C11$	
403vs			389	vC10-C12	391	vC9-C11 vC10-C12	382	$\delta N6C15N5$ $\delta N5C15N4$	
		363	$\delta C13N4C15$ $\tau wNH_2(N5)$	360	$\delta C13N4C15$ $\tau R_3(A1)$	353	$\delta C13N4C15$ $\tau R_3(A1)$		
337w	334	$\tau wNH_2(N6)$	325	wagNH <sub>2</sub> (N5)			325	$\delta N6C15N5$ $\delta N6C15N4$	

	314	$\beta$ C7-C8 $\beta$ C10-C12 $\beta$ C9-C11	309	$\beta$ C7-C8	313	$\beta$ C7-C8 $\beta$ C9-C11 $\beta$ C10-C12	305	$\tau$ wNH <sub>2</sub>
289w	279	$\gamma$ C9-C11 $\gamma$ C10-C12			282	$\gamma$ C10-C12 $\gamma$ C9-C11	290	$\rho$ C13=O3 $\delta$ N6C15N4 $\delta$ N5C15N4
			270	$\gamma$ C9-C11 $\gamma$ C10-C12	276	wagNH <sub>2</sub> (N6)	271	$\delta$ N6C15N5
259m			242	$\tau$ wNH <sub>2</sub> (N5)	247	$\delta$ C8C13N4		
226m	238	$\beta$ C10-C12 $\beta$ C9-C11	236	$\beta$ C9-C11	227	vH25-C126	217	$\delta$ N6C15N4 $\delta$ N5C15N4
197s	199	$\tau$ R <sub>2</sub> (A1)	198	$\tau$ R <sub>3</sub> (A1)	199	$\tau$ R <sub>3</sub> (A1)	199	$\tau$ R <sub>2</sub> (A1) $\tau$ R <sub>3</sub> (A1)
186sh					196	vH25-C126 $\beta$ C9-C11		
174sh	178	$\delta$ C8C13N4	175	$\delta$ C8C13N4 $\beta$ C10-C12				
	140	$\tau$ N4-C15					157	$\delta$ N5C15N4
119s			109	$\tau$ C13-N4 $\tau$ N4-C15			124	$\tau$ C13-N4
119s			105	$\tau$ N4-C15	102	vH25-C126 $\tau$ R <sub>3</sub> (A1)		
86s	94	$\tau$ R <sub>3</sub> (A1)			99	$\tau$ C13-N4	94	$\delta$ N6C15N4 $\tau$ R <sub>3</sub> (A1)
86s			83	$\tau$ C13-N4	82	$\tau$ N4-C15		
64vs	73	$\tau$ C13-N4			71	$\delta$ N4H25C126		
64vs	55	$\delta$ C7C8C13 $\gamma$ C7-C8	55	$\delta$ C7C8C13 $\gamma$ C7-C8	58	wagNH <sub>2</sub> (N5)	59	$\delta$ C7C8C13 $\gamma$ C7-C8
64vs					49	$\delta$ C7C8C13 $\gamma$ C7-C8		
16vw	18	$\tau$ C8-C13	26	$\tau$ wC8-C7			38	$\tau$ wC8-C7
16vw	14	$\tau$ wC8-C7	14	$\tau$ C8-C13	16	$\tau$ wC8-C7	19	$\tau$ C8-C13
3w					9	$\tau$ C8-C13	12	$\tau$ N4-C15

Abbreviations: v, stretching;  $\beta$ , deformation in the plane;  $\gamma$ , deformation out of plane; wag, wagging;  $\tau$ , torsion;  $\beta$ <sub>R</sub>, deformation ring  $\tau$ <sub>R</sub>, torsion ring;  $\rho$ , rocking;  $\tau$ w, twisting;  $\delta$ , deformation; a, antisymmetric; s, symmetric; (A<sub>1</sub>), Ring 1. <sup>a</sup>This work, <sup>b</sup>From scaled quantum mechanics force field, <sup>c</sup>From Ref [4], <sup>d</sup>From Ref [8].

### Band Assignments

**4000-2000 cm<sup>-1</sup> region.** In this region are expected the antisymmetric and symmetric stretching modes of NH<sub>2</sub> and CH<sub>2</sub> groups and also the stretching modes corresponding to the three aromatics C-H bonds belonging to free base B, cationic E, hydrochloride F and anionic D species of guanfacine. Besides, the N-H stretching modes of anionic, cationic and hydrochloride species are also expected. The SQM calculations predicted the two stretching modes of NH<sub>2</sub> groups to higher wavenumbers than the corresponding to CH<sub>2</sub> groups and, moreover, the antisymmetric modes at higher wavenumbers than the corresponding symmetrical. In the anionic species, the N-H stretching modes is predicted at 3188 cm<sup>-1</sup> while in the cationic and hydrochloride species these modes are predicted at 3454 and 2549 cm<sup>-1</sup>, respectively. Hence, the absence of the band predicted at 2549 cm<sup>-1</sup> in the experimental spectrum clearly indicate that the hydrochloride species is not presents in the solid phase. The

assignments of all these modes were performed as predicted by SQM calculations and, as was detailed in Table 7.

**2000-1000  $cm^{-1}$  region.** This region is characteristic of C=O, C-C and C-N stretching modes, deformation and rocking modes of  $NH_2$  and  $CH_2$  groups, wagging modes of  $CH_2$  groups, rocking modes of C-H and N-H groups and, some deformations of dichlorophenyl rings can also be observed. Thus, the IR band at  $1700\text{ cm}^{-1}$ , observed in the Raman spectrum at  $1751\text{ cm}^{-1}$ , is clearly assigned to the C13=O3 stretching modes of cationic and hydrochloride species. Note that the free base and the anionic species are predicted at lower wavenumbers. Here, both C15-N5 and C15-N6 stretching modes of the cationic species are predicted with double bond characters at  $1687\text{ cm}^{-1}$  (C=N) indicating that the cationic species E is the same than the cationic G because these species have the same reactivities and solvation energies in solution (see Scheme 1 and Tables 2 and 6). Therefore, the IR band at  $1690\text{ cm}^{-1}$  is simultaneously assigned to C=N stretching modes, deformation  $NH_2$  and rocking N-H modes, among other. For all species of Table 7, the C=C stretching modes corresponding to dichlorophenyl rings are predicted between  $1583$  and  $1562\text{ cm}^{-1}$  and, for this reason, they are assigned in these regions.

**1000-10  $cm^{-1}$  region.** Here, for the species of guanfacine some C-C, C-N and C-Cl stretching, other C-H, C-C and C=O deformations out-of-plane, wagging and twisting  $NH_2$ , twisting  $CH_2$  and deformations and torsions of dichlorophenyl rings modes are expected. The assignments for those modes were performed as predicted by SQM calculations and by comparison with species containing similar groups [18-25,34-44]. The assignments detailed of those modes are presented in Table 7.

### Force Fields

The force constants are interesting parameters that describe the force and characteristics of different bonds, hence, the knowledge of these factors in the guanfacine species are very useful to identify the nature of different C15-N4, C15-N5 and C15-N6 bonds because the double or simple bond character of these bonds change in the free base, cationic, hydrochloride and anionic species. Therefore, the harmonic force constants were calculated for all species of guanfacine by using the 6-31G\* method and the corresponding harmonic force fields expressed in internal coordinates. First, the harmonic force fields were computed in Cartesian coordinates with the SQMFF procedure [28] and the Molvib program [30] and, then, they were converted

to internal coordinates. In **Table 8** are given the scaled force constants for five species of guanfacine in gas phase compared with those reported for the corresponding species of gramine alkaloid in the same medium [50].

**Table 8. Scaled internal force constants for the most stable anionic, free base, cationic and hydrochloride species of guanfacine by using the B3LYP/6-31G\* method.**

Force constant	Guanfacine <sup>a</sup>				Gramine <sup>b</sup>		
	Free base B	Cationic E	HCl F	Anionic D	Free base	Cationic	HCl
$f(\nu NH_2)$	6.56	6.58	6.04	6.39			
$f(\nu C=O)$	10.48	12.18	11.38	10.53			
$f(\nu N-H)$		6.60	4.50	5.65		6.00	2.80
$f(\nu C-N)$	7.08	7.06	7.44	6.73	6.15	6.30	6.25
$f(\nu CH_2)$	4.91	4.82	4.88	4.93	4.48	4.92	4.82
$f(\nu C-H)_R$	5.23	5.26	5.24	5.18	5.18	5.20	5.18
$f(\nu C=C)$	6.55	6.56	6.55	6.50	7.30	7.00	7.20
$f(\nu C-C)$	4.04	4.14	4.13	3.51	4.50	4.90	4.70
$f(\delta CH_2)$	0.75	0.74	0.74	0.75	0.80	0.80	0.80

Units are mdyn Å<sup>-1</sup> for stretching and mdyn Å rad<sup>-2</sup> for angle deformations

<sup>a</sup>This work, <sup>b</sup>From Ref [50], HCl= Hydrochloride species

Analysing first the force constants for the five guanfacine species, we observed that  $f(\nu NH_2)$  force constant for the cationic species shows the higher value because in this species the charge is located on the N atom of N-H group while in the hydrochloride species the charge is neutralized due to Cl atom. Probably, the proximity of Cl atom to a NH<sub>2</sub> group diminishes the corresponding force constant. In relation to the  $f(\nu C=O)$  force constants, the cationic species presents the higher value because the B3LYP/6-31G\* calculations predicted the lower C=O distance for this species while in the anionic species the higher distance clearly justify the low force constant value. Here, the  $f(\nu N-H)$  force constant for the cationic species presents the higher value while in the hydrochloride species the force constant value quickly decrease due to Cl atom. In this hydrochloride species, the N-H bond is most weak due to that the H atom is linked to Cl atom by means of an ionic interaction and, hence, the force constant value is low compared with the cationic one. This result is also observed in the species of gramine and cyclizine [24,50]. Evaluating the  $f(\nu C-H)_R$  force constants corresponding to the dichlorophenyl rings and the  $f(\nu C-N)$ ,  $f(\nu C=C)$  and  $f(\nu C-C)$  force constants of all species, it is clearly observed that the anionic D species presents the lower values possibly due to the negative charge on O atom that generates modifications in its structure and, for these reasons, changes in the force constants values are observed. When the force constants values for guanfacine species are

compared with the reported for the gramine species it is observed that the  $f(\nu_{C-N})$  force constants of guanfacine are higher than the corresponding to gramine while, on the contrary, the  $f(\nu_{C=C})$  force constants of gramine species are higher than the guanfacine species. These latter results can easily be justified because in the gramine species the phenyl ring is fused to indol ring. In general, the  $f(\nu_{CH_2})$  and  $f(\delta_{CH_2})$  force constants are in concordance with values reported in the literature for compounds with similar groups [18-25,34-44,50-52].

## CONCLUSION

In the present work, the molecular structures of three tautomeric forms of free base (A, B and C), two cationic (E and G), one anionic D and two hydrochloride (F and H) species of antihypertensive agent guanfacine were theoretically determined in gas phase and in aqueous solution by using the hybrid B3LYP/6-31G\* method. The structures of all species in solution were optimized with the polarized continuum (PCM) model while the corrected solvation energies were computed with the universal solvation model. The optimizations of tautomeric free bases have evidenced that the three A, B and C species are different in gas phase while in aqueous solution the species B and C presenting the same energies, volume and dipole moment values but the variations in its corrected solvation energy values by ZPVE indicating clearly that B is different from C. On the other hand, the two cationic species E and G have the same energy values in both media but different dipole moment values in gas phase are observed. Besides, G has evidenced imaginary frequency in gas phase. In solution, both species could be the same although the volumes are slightly different between them. In relation to both hydrochloride species, F exists in gas phase while H in aqueous solution. The anionic D species in both media presents positive frequencies while in solution exists when the enol OH group in the tautomeric form C is deprotonated in alkaline medium, as was suggested experimentally [2]. The comparisons among the predicted geometrical parameters and the corresponding experimental ones have evidenced good correlations in the bond lengths and angles, however, significant differences in the dihedral angles are observed.

The higher corrected solvation energy value is observed for the anionic species of guanfacine with a valor of -301,60 kJ/mol, slightly lower than the corresponding to scopolamine alkaloid (-310.34 J/mol) and higher than the corresponding to cocaine alkaloid (-255.24 J/mol). The frontier orbitals studies have evidenced that in gas phase, the anionic D species has the lowest gap value and, for this reason, it species is the most reactive while in solution the hydrochloride H species is the most reactive together with the anionic species. High global nucleophilicity

(E) and electrophilicity indexes ( $\omega$ ) values have showed both cationic species E and G while the lower values of those two indexes are predicted for the anionic D species in both media. In addition, the harmonic force fields, force constants and the complete vibrational assignments for the 63, 66, 69 and 72 vibration normal modes expected for the anionic, free bases, cationic and hydrochloride species of guanfacine are respectively reported for first time.

## ACKNOWLEDGEMENTS

This work was supported with grants from CIUNT Project N° 26/D608 (Consejo de Investigaciones, Universidad Nacional de Tucumán). The authors would like to thank Prof. Tom Sundius for his permission to use MOLVIB.

## REFERENCES

- [1] Sorkin, EM.; Heel, RC. Guanfacine. A review of its pharmacodynamic and pharmacokinetic properties, and therapeutic efficacy in the treatment of hypertension, *Drugs*, 1986, 31(4): 301-336.
- [2] Tomas A, Viossat B, Charlot MF, Girerd JJ. Dung Nguyen Huy, Tautomeric changes in guanfacine and its copper(II) complex as revealed by X-ray crystallography; synthesis and EPR, *Inorganica Chimica Acta*, 2005, 358: 3253-3258.
- [3] Brunton LL, Parker KL, Lazo JS. Goodman & Gilman's the pharmacological basis of therapeutics (11th ed. edición). New York: McGraw-Hill Medical Publishing Division. 2005, p. 256. ISBN 0-07-142280-3.
- [4] Xiao-Hua J, Jin-Zhao J, Hui Z, Bao-Ming L. Stimulation of  $\alpha_2$ -Adrenoceptors Suppresses Excitatory Synaptic Transmission in the Medial Prefrontal Cortex of Rat, *Neuropsychopharmacology*, 2008, 33: 2263–2271.
- [5] Tünde Jurca, EM, Florin B. Interaction of Metal Ions with Guanfacine, *REV. CHIM. (Bucharest)*, 2010, 61(5): 487-490.
- [6] Amy F.T. Arnsten, Lu E. Jin, Guanfacine for the treatment of cognitive disorders: A century of discoveries at Yale, *Yale J. Biology and Medicine*, 2012, 85: 45-58.
- [7] Briggs GG, Yaffe SJ, Freeman RK. *Drugs in pregnancy and lactation: a reference guide to fetal and neonatal risk* (10a edición). 2015, 1829-1830. ISBN 978-1-4511-9082-3.
- [8] Tünde Junca, EM, Grația Vicaș L, Mureșan, ME, Fritea, L. Metal Complexes of Pharmaceutical Substances, *Intech Open*, Chapter 7, Spectroscopic Analyses- Developments and Applications, 2017, 123-142.
- [9] Li A, Yeo K, Welty D, Rong H. Development of Guanfacine Extended-Release Dosing Strategies in Children and Adolescents with ADHD Using a Physiologically Based Pharmacokinetic Model to Predict Drug-Drug Interactions with Moderate CYP3A4 Inhibitors or Inducers, *Pediatric Drugs*, 2017, 20(2): 181-194.
- [10] Sandiego CM, Matuskey D, Lavery M, McGovern E, Huang Y, Nabulsi N, Ropchan J, Picciotto MR, Morris ED, McKee SA, Cosgrove KP. The Effect of Treatment with Guanfacine, an Alpha2 Adrenergic Agonist, on Dopaminergic Tone in Tobacco Smokers: An [11C]FLB457 PET Study, *Neuropsychopharmacology*, 2017, 43(5): 1052-1058.
- [11] Nishitomi K, Yano K, Kobayashi M, Jino K, Kano T, Horiguchi N, Shinohara S, Hasegawa M. Systemic administration of guanfacine improves food-motivated impulsive choice behavior primarily via direct stimulation of postsynaptic  $\alpha_2A$  -adrenergic receptors in rats, *Behavioural Brain Research*, 2018, 345: 21-29.
- [12] Haney M, Cooper, Ziva D, Bedi G, Herrmann E, Comer SD, Reed SC, Foltin RW, Levin FR. Guanfacine decreases symptoms of cannabis withdrawal in daily cannabis smokers, *Addiction Biology*, 2018. <https://doi.org/10.1111/adb.12621>
- [13] Molife C, Haynes VS, Nyhuis A, Faries DE, Gelwicks S, Kelsey DK, Alatorre CI. Healthcare utilization and costs of children with attention deficit/hyperactivity disorder initiating atomoxetine versus extended-release guanfacine, *Current Medical Research and Opinion*, 2018, 34(4): 619-632.

- [14] Okada BK, Li A, Seyedsayamdost MR. Identification of the Hypertension Drug Guanfacine as an Antivirulence Agent in *Pseudomonas aeruginosa*, *ChemBioChem*, 2019, 10.1002/cbic.201900129.
- [15] Neri LC, Johansen HL, Hewitt D, Marier J, Langner N. Magnesium and Certain Other Elements and Cardiovascular Disease, *Sci. Total Environ.*, 1985, 42: 49–75.
- [16] Kendrick MJ, May MT, Plishka MJ, Robinson KD. *Metals in Biological Systems*, Ellis Horwood, New York, 1992.
- [17] Chobanian AV, Bakris GL, Black HR, Cushman WC, Green LA, Izzo, Jr, JL, Jones DW, Materson BJ, Oparil S, Wright JT, Jr, Roccella EJ. The National High Blood Pressure Education Program Coordination Committee: Seventh Report of the Joint National Committee on Prevention, Detection, Evaluation and Treatment of High Blood Pressure, *Hypertension*, 2003, 42: 1206–1252.
- [18] Brandán SA. Why morphine is a molecule chemically powerful. Their comparison with cocaine. *Indian Journal of Applied Research*, 2017, 7(7): 511-528.
- [19] Rudyk R., Brandán SA. Force field, internal coordinates and vibrational study of alkaloid tropane hydrochloride by using their infrared spectrum and DFT calculations. *Paripex A Indian Journal of Research*, 2017, 6(8): 616-623.
- [20] Romani D, Brandán SA. Vibrational analyses of alkaloid cocaine as free base, cationic and hydrochloride species based on their internal coordinates and force fields. *Paripex A Indian Journal of Research*, 2017.6(9): 587-602.
- [21] Brandán SA. Understanding the potency of heroin against to morphine and cocaine. *IJSRM*, 2018, 12(2): 97-140.
- [22] Rudyk RA, Checa MA, Guzzetti KA, Iramain MA, Brandán SA. Behaviour of N-CH<sub>3</sub> Group in Tropane Alkaloids and correlations in their Properties. *IJSRM*, 2018; 10 (4): 70-97.
- [23] Iramain MA, Brandán SA. Structural and vibrational properties of three species of anti-histaminic diphenhydramine by using DFT calculations and the SQM approach. *Journal: To Chemistry Journal*, 2018, 1(1): 105-130.
- [24] Márquez MJ, Iramain MA, Brandán SA. *Ab-initio* and Vibrational studies on Free Base, Cationic and Hydrochloride Species Derived from Antihistaminic Cyclizine agent. *IJSRM*, 2018, 12(2): 97-140.
- [25] Manzur ME, Rudyk RA, Brandán SA. Evaluating properties of free base, cationic and hydrochloride Species of potent psychotropic 4-Bromo-2,5-dimethoxyphenethylamine drug, *International Journal of Current Advanced Research*, 8(3) (2019) 17166-17170.
- [26] Becke AD. Density-functional exchange-energy approximation with correct asymptotic behavior. *Phys. Rev.*, 1988, A38: 3098-3100.
- [27] Lee C, Yang W, Parr RG. Development of the Colle-Salvetti correlation-energy formula into a functional of the electron density. *Phys. Rev.*, 1988, B37: 785-789.
- [28] Pulay P, Fogarasi G, Pongor G, Boggs JE, Vargha A. Combination of theoretical ab initio and experimental information to obtain reliable harmonic force constants. Scaled quantum mechanical (SQM) force fields for glyoxal, acrolein, butadiene, formaldehyde, and ethylene. *J. Am. Chem. Soc.*, 1983, 105: 7073.
- [29] a) Rauhut G, Pulay P. Transferable Scaling Factors for Density Functional Derived Vibrational Force Fields. *J. Phys. Chem.*, 1995, 99: 3093-3100. b) *Correction*: Rauhut G, Pulay P. *J. Phys. Chem.*, 1995, 99: 14572.
- [30] Sundius T. Scaling of ab-initio force fields by MOLVIB. *Vib. Spectrosc.*, 2002, 29 : 89-95.
- [31] Miertus S, Scrocco E, Tomasi J. Electrostatic interaction of a solute with a continuum. *Chem. Phys*, 1981, 55: 117–129.
- [32] Tomasi J, Persico J. Molecular Interactions in Solution: An Overview of Methods Based on Continous Distributions of the Solvent. *Chem. Rev.*, 1994, 94: 2027-2094.
- [33] Marenich AV, Cramer CJ, Truhlar DG. Universal solvation model based on solute electron density and a continuum model of the solvent defined by the bulk dielectric constant and atomic surface tensions. *J. Phys. Chem.*, 2009, B113: 6378-6396.
- [34] Chain F, Romano E, Leyton P, Paipa C, Catalán CAN, Fortuna MA, Brandán SA. An experimental study of the structural and vibrational properties of sesquiterpene lactone cnicin using FT-IR, FT-Raman, UV–visible and NMR spectroscopies. *J. Mol. Struct.* 2014, 1065-1066: 160-169.
- [35] Romani D, Brandán SA, Márquez MJ, Márquez MB. Structural, topological and vibrational properties of an isothiazole derivatives series with antiviral activities. *J. Mol. Struct.*, 2015, 1100: 279-289.

- [36] Chain F, Ladetto MF, Grau A, Catalán CAN, Brandán SA. Structural, electronic, topological and vibrational properties of a series of N-benzylamides derived from Maca (*Lepidium meyenii*) combining spectroscopic studies with ONION calculations. *J. Mol. Struct.* 2016, 1105: 403-414.
- [37] Romani D, Tsuchiya S, Yotsu-Yamashita M, Brandán SA. Spectroscopic and structural investigation on intermediates species structurally associated to the tricyclic bisguanidine compound and to the toxic agent, saxitoxin. *J. Mol. Struct.*, 2016, 1119: 25-38.
- [38] Romano E, Castillo MV, Pergomet JL, Zinczuk J, Brandán SA. Synthesis, structural and vibrational analysis of (5,7-Dichloro-quinolin-8-yloxy) acetic acid. *J. Mol. Struct.*, 2012, 1018: 149–155.
- [39] Issaoui N, Ghalla H, Brandán SA, Bardak F, Flakus HT, Atac A, Oujia B. Experimental FTIR and FT-Raman and theoretical studies on the molecular structures of monomer and dimer of 3-thiopheneacrylic acid. *J. Mol. Struct.*, 2017, 1135: 209-221.
- [40] Minteguiaga M, Dellacassa E, Iramain MA, Catalán CAN, Brandán SA. A structural and spectroscopic study on carquejol, a relevant constituent of the medicinal plant *Baccharis trimera* (Less.) DC. (Asteraceae). *J. Mol. Struct.* 2017, 1150: 8-20.
- [41] Minteguiaga M, Dellacassa E, Iramain MA, Catalán CAN, Brandán SA. FT-IR, FT-Raman, UV-Vis, NMR and structural studies of Carquejyl Acetate, a component of the essential oil from *Baccharis trimera* (Less.) DC. (Asteraceae). *J. Mol. Struct.* 2018, 1177: 499-510.
- [42] Minteguiaga M, Dellacassa E, Iramain MA, Catalán CAN, Brandán SA. Synthesis, spectroscopic characterization and structural study of 2-isopropenyl-3-methylphenol, carquejiphenol, a carquejol derivative with potential medicinal use. *J. Mol. Struct.*, 2018, 1165: 332-343.
- [43] Rudyk RA, Checa MA, Catalán CAN, Brandán SA. Structural, FT-IR, FT-Raman and ECD spectroscopic studies of free base, cationic and hydrobromide species of scopolamine alkaloid. *J. Mol. Struct.* , 2019, 1180: 603-617.
- [44] Iramain MA, Davies L, Brandán SA. Structural and spectroscopic differences among the Potassium 5-hydroxypentanoyltrifluoroborate salt and the furoyl and isonicotinoyl salts. *J. Mol. Struct.*, 2019, 1176: 718-728.
- [45] Nielsen AB, Holder AJ. Gauss View 3.0. User's Reference, GAUSSIAN Inc., Pittsburgh, PA, 2000–2003.
- [46] Frisch MJ, Trucks GW, Schlegel HB, Scuseria GE, Robb MA, Cheeseman JR, Scalmani G, Barone V, Mennucci B., Petersson GA, Nakatsuji H, Caricato M, Li X, Hratchian HP, Izmaylov AF, Bloino J, Zheng G, Sonnenberg JL, Hada M, Ehara M, Toyota K, Fukuda R, Hasegawa J, Ishida M, Nakajima T, Honda Y, Kitao O, Nakai H, Vreven T, Montgomery JA, Peralta JE, Ogliaro F, Bearpark M, Heyd JJ, Brothers E, Kudin KN, Staroverov VN, Kobayashi R, Normand J, Raghavachari K, Rendell A, Burant JC, Iyengar SS, Tomasi J, Cossi M, Rega N, Millam JM, Klene M, Knox JE., Cross JB, Bakken V, Adamo C, Jaramillo J, Gomperts R, Stratmann RE, Yazyev O, Austin AJ, Cammi R, Pomelli C, Ochterski JW, Martin RL, Morokuma K, Zakrzewski VG, Voth GA, Salvador P, Dannenberg JJ, Dapprich S, Daniels AD, Farkas O, Foresman JB, Ortiz J., Cioslowski J, Fox DJ. Gaussian, Inc., Wallingford CT, 2009.
- [47] Ugliengo P. Moldraw Program, University of Torino, Dipartimento Chimica IFM, Torino, Italy, 1998.
- [48] Keresztury G, Holly S, Besenyi G, Varga J, Wang AY, Durig JR. Vibrational spectra of monothiocarbamates-II. IR and Raman spectra, vibrational assignment, conformational analysis and ab initio calculations of S-methyl-N,N-dimethylthiocarbamate. *Spectrochim. Acta*, 1993, 49A: 2007-2026.
- [49] Michalska D, Wysokinski. The prediction of Raman spectra of platinum(II) anticancer drugs by density functional theory. *Chemical Physics Letters*, 2005, 403: 211-217.
- [50] Iramain MA, Ruiz Hidalgo J, Brandán SA. Predicting properties of species derived from N-(1H-indol-3-ylmethyl)-N,N-dimethylamine, Gramine, a indol alkaloid, *International Journal of Current Advanced Research*, 8(4) (2019) 18113-18124.
- [51] Iramain MA, Ruiz Hidalgo J, Brandán SA. Effect of media on the properties of monoterpene cyclic Eucalyptol, *IJSRM*, 2019, 12(3): 70-101.
- [52] Manzur ME, Brandán SA. S(-) and R(+) Species Derived from Antihistaminic Promethazine Agent: Structural and Vibrational Studies, Submitted to *Heliyon* (2019).
- [53] Parr RG, Pearson RG. Absolute Hardness: companion parameter to absolute electronegativity. *J. Am. Chem. Soc.*, 1983, 105: 7512-7516.